Interplay between new physics in one-loop Higgs couplings and the top-quark Yukawa coupling

Xiao-Gang He,[1,2,3,*] Yong Tang,[2,†] and German Valencia[4,‡]

[1]*INPAC, SKLPPC and Department of Physics, Shanghai Jiao Tong University, Shanghai 200240, China*
[2]*Department of Physics, National Tsing Hua University and National Center for Theoretical Sciences, Hsinchu 30013, Taiwan*
[3]*CTS, CASTS and Department of Physics, National Taiwan University, Taipei 10617, Taiwan*
[4]*Department of Physics, Iowa State University, Ames, Iowa 50011, USA*

(Received 17 June 2013; published 15 August 2013)

After the discovery of a 126 GeV state at the LHC, it is imperative to establish whether this particle really is the Higgs boson of the standard model. The early measurements have not yet pinpointed any of the Higgs couplings to fermions, the Yukawa couplings of the standard model. In this paper we study the values of the top-quark–Higgs coupling, $g_{ht\bar{t}}$, that are still allowed by the one-loop couplings of the Higgs to two gluons or two photons. We first assume that both the gluon fusion production of the Higgs and its decay into two photons proceed through loops with standard model particles only, albeit with an arbitrary top-Higgs coupling. We find that the current Higgs data still allow for 20% deviations in $g_{ht\bar{t}}$ from its standard model value. We then investigate the effect of new particles contributing to the effective one-loop couplings. Specifically, we consider a color-octet electroweak doublet extension of the scalar sector and find that, in this case, $g_{ht\bar{t}}$ is allowed to deviate from its standard model value by 40% with the current data.

DOI: 10.1103/PhysRevD.88.033005 PACS numbers: 14.80.Bn, 14.80.Ec, 14.65.Jk, 12.60.Fr

I. INTRODUCTION

The two collaborations ATLAS and CMS at the Large Hadron Collider (LHC) have found a new resonant state of mass near 126 GeV [1,2], purported to be the standard model (SM) Higgs boson. The immediate task after the discovery of this state it to establish whether it really is the Higgs boson of the standard model or whether there is physics beyond it (BSM). In particular, the early measurements have not yet ascertained any of the Higgs couplings to fermions, the Yukawa couplings of the standard model.

This leaves open the more general possibility of a symmetry breaking sector separate from a fermion mass generation sector as in the early technicolor models [3]. In general, even the scale of electroweak symmetry breaking and that of fermion mass generation need not coincide [4,5] and this motivates us to investigate deviations in the top-quark-Higgs coupling from its SM value. Of course, this possibility is not as exotic as it may first appear as even a simple two Higgs doublet model relaxes the proportionality between the fermion mass and its coupling to the (lightest) Higgs boson.

We will not concern ourselves with a detailed model of this kind. Instead we will be interested in the purely phenomenological question of constraining the values of the top-quark coupling to the observed Higgs boson using the current data. The main ingredients for this study are the one-loop couplings of the Higgs boson, namely its production via gluon fusion and its decay into two photons and into $Z\gamma$, as these modes involve a top-quark loop and therefore the top-quark-Higgs coupling. The experimental uncertainty in these measurements allows for a range of possible top-quark Yukawa couplings which we will discuss first.

We then study the interplay between the allowed range for the top-quark-Higgs coupling and BSM particles that can change the one-loop Higgs processes. In particular we will consider a simple extension of the scalar sector of the SM with new scalars S transforming as $(8, 2, 1/2)$ under the SM gauge group $SU(3)_C \times SU(2)_L \times U(1)_Y$. This color-octet, electroweak doublet, scalar extension of the SM is that of Ref. [6], motivated by the requirement of minimal flavor violation [7,8], and we have recently constrained the relevant parameters with unitarity and vacuum stability arguments [9].

II. MODIFIED TOP QUARK–HIGGS COUPLING

In the SM the top-quark coupling to the Higgs boson is uniquely determined by its mass as the Yukawa interaction reads

$$\mathcal{L}_{htt} = y_t \bar{q} t \tilde{\phi} + \text{H.c.}, \tag{2.1}$$

where q is the third generation SM quark doublet, ϕ is the scalar doublet, $\tilde{\phi}_i = \epsilon_{ij}\phi_j$, and the top-quark acquires a mass when electroweak symmetry is broken and the Higgs field develops a vacuum expectation value (VEV) $\langle\phi\rangle = v/\sqrt{2}$, $v \approx 246$ GeV. Equation (2.1) then leads to the couplings

$$\mathcal{L}_{htt} = \frac{y_t v}{\sqrt{2}} \bar{t}t\left(1 + \frac{h}{v}\right). \tag{2.2}$$

*hexg@phys.ntu.edu.tw
†ytang@phys.cts.nthu.edu.tw
‡valencia@iastate.edu

The $ht\bar{t}$ coupling, $g_{ht\bar{t}}$, is thus fixed by the top-quark mass as $g_{ht\bar{t}} = y_t/\sqrt{2} = m_t/v$.

Beyond the SM, however, this no longer holds. In a model independent manner we can describe physics BSM with an effective Lagrangian that respects the symmetries of the SM. If we accept the 126 GeV state observed at LHC as a fundamental scalar, the appropriate effective Lagrangian for BSM physics with terms up to dimension six is that of Buchmuller and Wyler [10,11]. One sees that already at dimension six there are terms in the Lagrangian modifying Eq. (2.1). For example, the term

$$\mathcal{L}_6 = \frac{g_{u\phi}}{\Lambda^2}(\phi^\dagger\phi)\bar{q}t\tilde{\phi} + \text{H.c.} \tag{2.3}$$

suffices to spoil the proportionality between the top-quark mass and its coupling to the Higgs boson. In the presence of this term the $ht\bar{t}$ coupling and the top-quark mass are modified to

$$\begin{aligned} g_{ht\bar{t}} &= \frac{y_t}{\sqrt{2}} + 3g_{u\phi}\frac{v^2}{2\sqrt{2}\Lambda^2} \\ m_t &= y_t\frac{v}{\sqrt{2}} + g_{u\phi}v\frac{v^2}{2\sqrt{2}\Lambda^2}. \end{aligned} \tag{2.4}$$

This equation illustrates how BSM the Higgs-top coupling $g_{ht\bar{t}}$ (Yukawa) depends on new physics (in this case the coupling $g_{u\phi}$) differently than the top-quark mass. Examples of specific models generating this operator would be: a tree-level exchange of a new heavy scalar singlet; or a one-loop exchange of two color-octet scalars discussed below when they are in a color singlet electroweak singlet configuration. We keep our discussion model independent and simply allow for an arbitrary $ht\bar{t}$ coupling parametrized by r_t defined by

$$\mathcal{L}_{\text{eff}} = r_t\frac{m_t}{v}\bar{t}th. \tag{2.5}$$

We thus have $g_{ht\bar{t}} = (g_{ht\bar{t}})_{\text{SM}}\, r_t$.

III. COLOR-OCTET SCALARS

To alter the loop induced couplings of the Higgs boson, we will consider a model in which the scalar sector is augmented with a color-octet, electroweak doublet in keeping with minimal flavor violation [6]. The phenomenology of this model has been studied extensively [9,12–25] so we keep its discussion to a minimum. The inclusion of the new multiplet S introduces several new, renormalizable, interaction terms to the Lagrangian. Because S has nontrivial $SU(3)_C \times SU(2)_L \times U(1)_Y$ quantum numbers, it will have corresponding gauge interactions. In addition there will be new terms in the Yukawa couplings and in the Higgs potential that are consistent with minimal flavor violation. Only three of the nine new parameters will affect our discussion in this paper and they appear in the scalar potential of Ref. [6] as

$$\begin{aligned} V = {} & \lambda\left(H^{\dagger i}H_i - \frac{v^2}{2}\right)^2 + 2M_S^2\,\text{Tr}S^{\dagger i}S_i + \lambda_1 H^{\dagger i}H_i\,\text{Tr}S^{\dagger j}S_j \\ & + \lambda_2 H^{\dagger i}H_j\,\text{Tr}S^{\dagger j}S_i + (\lambda_3 H^{\dagger i}H^{\dagger j}\,\text{Tr}S_iS_j + \text{H.c.}) \\ & + \cdots \end{aligned} \tag{3.1}$$

The first term is the same as the SM scalar potential and we use the conventional definition of λ and of $v \sim 246$ GeV. The traces are over the color indices and the $SU(2)$ indices i, j are displayed explicitly.

For our numerical discussion we will eliminate λ_3 by using the custodial symmetry relation $2\lambda_3 = \lambda_2$. We will also restrict the ranges of λ_1 and λ_2 according to their recently derived unitarity and vacuum stability constraints. In particular, we will use the following two conditions:

(i) the tree-level unitarity constraint as described in Ref. [9], which can be summarized by

$$|2\lambda_1 + \lambda_2| \lesssim 18. \tag{3.2}$$

(ii) the renormalization group improved (RGI) unitarity constraint of the coupled equations for λ, λ_1, and λ_2, satisfied up to a large scale of 10^{10} GeV. This produces an allowed region shown in Fig. 3 of Ref. [9], which we import for this paper (the blue region in Fig. 2). Roughly, it can be thought of as the area limited by $-1.5 \lesssim \lambda_1 \lesssim 1.2$ and $-1.7 \lesssim \lambda_2 \lesssim 1.2$.

The masses of the scalars contributing to the one-loop Higgs couplings to gluons and photons are given in terms of the parameters of Eq. (3.1) by [6]

$$\begin{aligned} m_{S^\pm}^2 &= m_S^2 + \lambda_1\frac{v^2}{4}, \\ m_{S_R^0}^2 &= m_S^2 + (\lambda_1 + \lambda_2 + 2\lambda_3)\frac{v^2}{4}, \\ m_{S_I^0}^2 &= m_S^2 + (\lambda_1 + \lambda_2 - 2\lambda_3)\frac{v^2}{4}. \end{aligned} \tag{3.3}$$

Their contribution to the effective couplings is reviewed in the Appendix. Our use of the custodial symmetry relations guarantees that the electroweak precision observable vanishes, $T = 0$, yielding no new constraints. The parameter S is known to receive the contribution $S = \frac{\lambda_2}{6\pi}\frac{v^2}{m_S^2}$ [6]. With reference values, $m_h = 125$ GeV and $m_t = 173$ GeV, $S|_{U=0} = 0.05 \pm 0.09$ [26], so that $\lambda_2 \sim 10$ is still allowed at 1σ for $m_s = 500$ GeV. This is comparable to Eq. (3.2) and much weaker than the RGI constraint.

IV. NUMERICAL RESULTS

Fits to the LHC Higgs data already exist in the literature [27–59] and we use Ref. [54] for our discussion. The relevant results from that reference are the fits to the one-loop effective couplings r_γ and r_g defined by

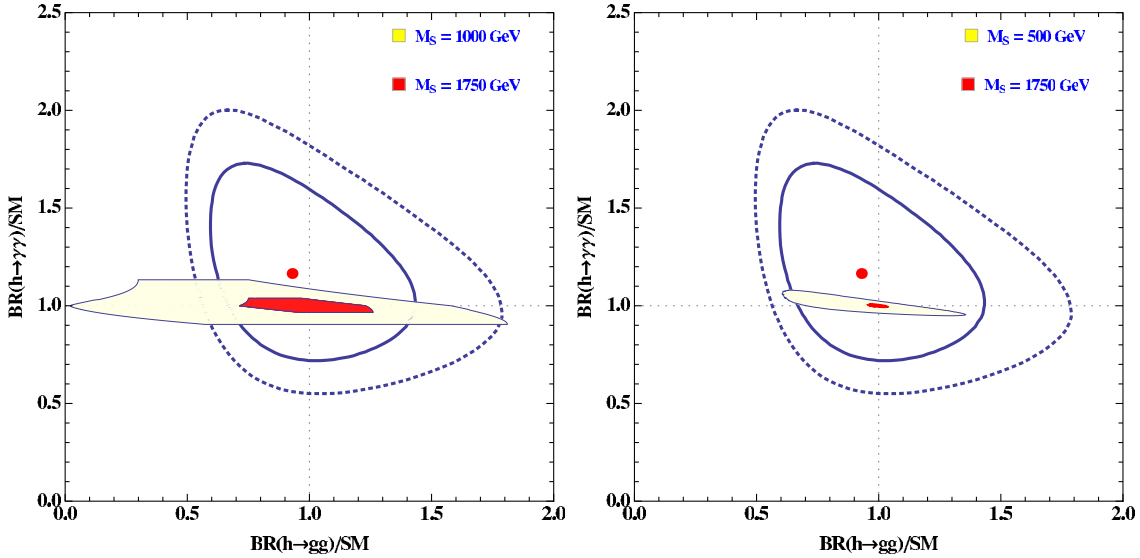

FIG. 1 (color online). Best fit to BR($h \to \gamma\gamma$) vs BR($h \to gg$) from Ref. [54]: the red dot is the best fit, the solid and dashed curves show the 1σ and 2σ allowed regions, respectively. In the left panel we have superimposed the range of predictions in the color-octet model for two values of M_S and values of $\lambda_{1,2}$ spanning the parameter space allowed by tree-level unitarity. In the right panel we span the parameter space allowed by the RGI unitarity conditions up to 10^{10} GeV.

$$\mathcal{L}_{hgg,h\gamma\gamma} = r_\gamma c_{\rm SM}^\gamma \frac{\alpha}{\pi v} h F_{\mu\nu} F^{\mu\nu} + r_g c_{\rm SM}^g \frac{\alpha_s}{12\pi v} h G^a_{\mu\nu} G^{a\mu\nu}, \quad (4.1)$$

where the SM contributions $c_{\rm SM}^\gamma$ and $c_{\rm SM}^g$ are reviewed in the Appendix.

A. Color-octet scalars

In Fig. 1 we show the results of the fit from Ref. [54], the red dot corresponding to the best fit to the data and the solid and dashed contours being the 1σ and 2σ regions, respectively. The SM is the point (1,1) in this plot as both axes are normalized to the SM rates. We have superimposed to this figure the results of adding a scalar color octet. The figure on the left shows the regions obtained with parameters λ_1 and λ_2 that satisfy the tree-level unitarity constraint. We illustrate two cases, the yellow (larger) region for $M_S = 1$ TeV and the red (smaller) region for $M_S = 1.75$ TeV. As expected, the region of possible rates shrinks as M_S increases and approaches the SM point. The figure on the right is obtained with parameters λ_1 and λ_2 that satisfy the RGI unitarity conditions up to a scale of 10^{10} GeV. Again, we have illustrated two regions: a larger yellow one corresponding to $M_S = 0.5$ TeV; and a smaller red one for $M_S = 1.75$ TeV. We see that for values of λ_1 and λ_2 satisfying the RGI conditions up to a high scale, the corrections to the $h \to gg$ and $h \to \gamma\gamma$ rates are always within (or very close to) the 1σ fit to LHC data.

We can turn the argument around and use the measured BR($h \to \gamma\gamma$) and BR($h \to gg$) to place additional constraints on the parameters $\lambda_1 - \lambda_2$ of the color-octet scalar potential. We show this result in Fig. 2. This figure reproduces the allowed parameter space from tree-level unitarity (yellow) and RGI unitarity up to 10^{10} GeV (blue) from Ref. [9]. On it we superimpose in dark (light) red the regions allowed at 1σ (2σ) by the BR($h \to \gamma\gamma$) and BR($h \to gg$) fit assuming the top-quark coupling is as in

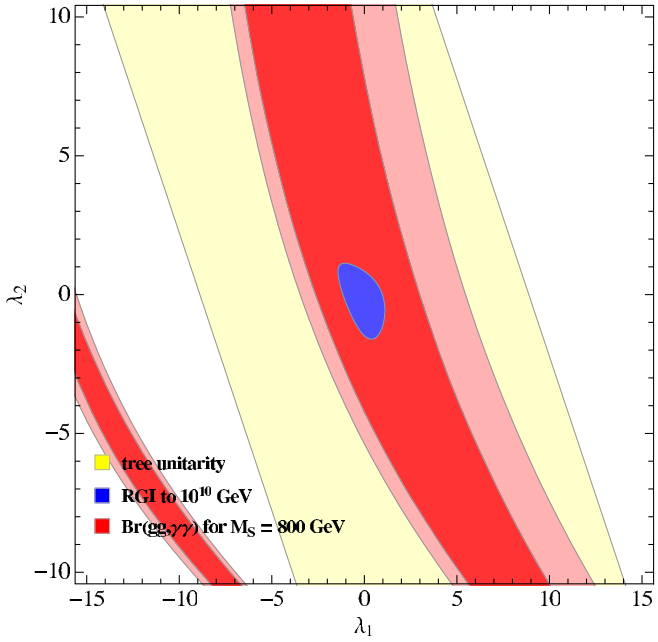

FIG. 2 (color online). Allowed $\lambda_1 - \lambda_2$ parameter space from Ref. [9] (yellow and blue regions as discussed in the text), superimposed with the regions allowed by the BR($h \to \gamma\gamma$) and BR($h \to gg$) at 1σ (dark red) and 2σ (light red).

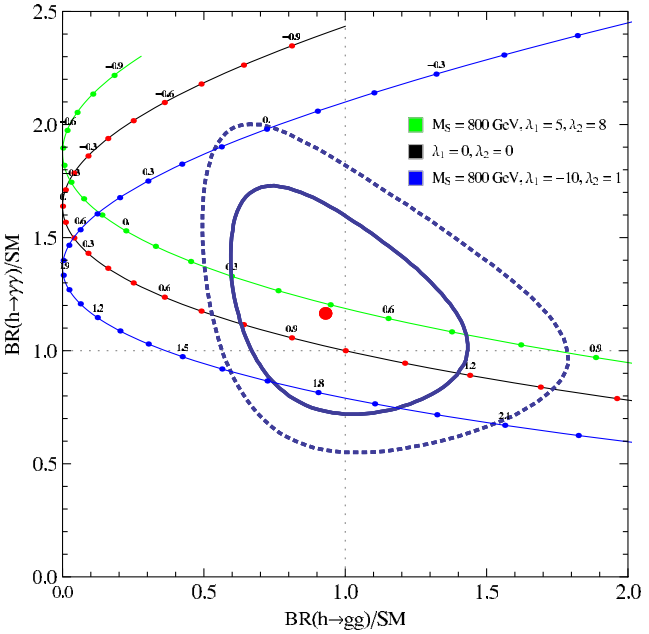

FIG. 3 (color online). BR($h \to \gamma\gamma$) vs BR($h \to gg$) as a function of r_t (dots along the curves) for three cases. The parameters chosen for the black curve correspond to no additional scalars.

the SM. The two separate regions correspond to constructive (upper, larger regions) and destructive interference (lower narrow regions) with the SM, respectively.

B. Allowed range for $ht\bar{t}$ coupling

We next consider the possibility of an arbitrary top-quark coupling to the Higgs boss, r_t, and illustrate three cases in Fig. 3. The black curve shows the rates obtained by allowing r_t to differ from 1 but without additional scalars (hence $\lambda_{1,2} = 0$). We see that at the 1σ level, the data permits a 20% excursion from the SM value, as the range $0.8 \lesssim r_t \lesssim 1.2$ is allowed. We also see that there are negative values of r_t close to the 2σ contour at higher BR($h \to \gamma\gamma$)/SM ~ 2.2. In fact, taking the ATLAS data alone there is a second allowed range $r_t \in [-0.88, -0.75]$ [60]. Notice that for $r_t = 1$, which is the SM, the values for BR($h \to \gamma\gamma$) and BR($h \to gg$) are not the closest point to the best fit values to data. In the SM (no color octet), the amplitude for $h \to \gamma\gamma$ has contributions from a W loop and a top loop with different signs and with the latter being proportional to r_t. Allowing r_t to be smaller than 1, the cancellation between W and top-quark loops is reduced resulting in a larger branching ratio for $h \to \gamma\gamma$ and therefore in a better fit to the data. If one only considers this decay mode, $r_t \sim 0.6$ corresponds to the central value of the fit. However, varying r_t will also modify $h \to gg$ whose amplitude is proportional to it. Taking both rates into account, the best fit is closer to $r_t \sim 0.95$.

New physics contributing to the loop amplitudes, such as the color-octet scalars, modifies the allowed r_t range and we illustrate this with the green and blue curves in Fig. 3. Values of $\lambda_{1,2}$ satisfying the RGI condition up to 10^{10} GeV result in minimal modifications, so we show two cases in which $\lambda_{1,2}$ are only required to satisfy the tree-level unitarity bound. A reversal of sign in r_t is not allowed at the 2σ level.

We collect in Fig. 4 three views of the allowed parameter space in the color-octet model as a function of r_t such that the one-loop rates stay within the 1σ region of the fit. The larger regions (yellow) span the $\lambda_1 - \lambda_2$ parameter space allowed by tree level unitarity and the smaller regions (blue) span the $\lambda_1 - \lambda_2$ parameter space allowed by the RGI unitarity condition up to 10^{10} GeV. We display the allowed values of r_t for ranges in M_S, $2\lambda_1 + \lambda_2$ and λ_1. The last two are chosen because $h \to gg$ depends mostly on $2\lambda_1 + \lambda_2$, whereas $h \to \gamma\gamma$ depends mostly on λ_1. The plots illustrate how a deviation in r_t from one can be compensated by the presence of additional scalars in the loop to end up with rates matching the observed ones.

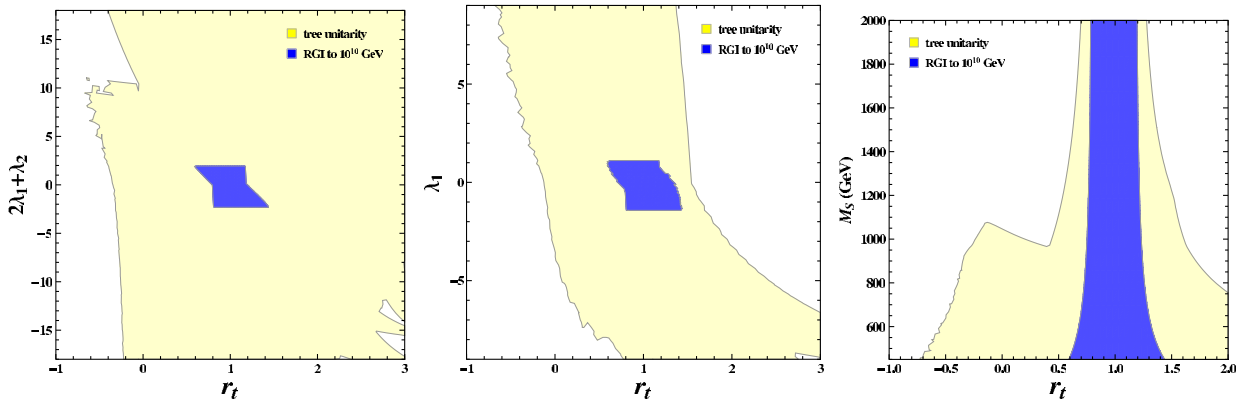

FIG. 4 (color online). Three views of the allowed parameter space at 1σ. The larger region (yellow) allowed by tree level unitarity and the smaller region (blue) allowed by the RGI unitarity condition up to 10^{10} GeV. We display the allowed values of r_t for ranges in $2\lambda_1 + \lambda_2$ (left) and λ_1 (center) and M_S (right).

V. OTHER MODES

In the previous discussion of constraints on the top quark coupling to Higgs, we have implicitly assumed that changing the top Yukawa coupling does not modify the fitted contours from Ref. [54]. This assumption is justified for the following reasons. The first one is that the main channel for Higgs production is gluon-gluon fusion in which the top quark only appears in the loop. In the decay channel, only Higgs to diphoton is involved with top. So the effects of changing the top coupling can be parametrized as $\mathrm{Br}(h \to gg)$ and $\mathrm{Br}(h \to \gamma\gamma)$. The second reason is that the direct measurement of the top Yukawa through $pp \to t\bar{t}h$ is not yet very restrictive, the current limit being about 5 times the SM value [61]. At present $r_t \in [-1, 1]$ is allowed by $pp \to t\bar{t}h$ alone. In addition, since the color-octet scalar does not develop a VEV, the tree-level hWW and hZZ couplings are not changed.

The introduction of a color octet, however, affects other loop induced processes such as $h \to Z\gamma$. We now study the predicted region allowed for this branching ratio. The detailed contributions are again reviewed in the Appendix. In general, the contribution from the new scalars to the decay $h \to \gamma\gamma$ is positively correlated with the contribution to $h \to Z\gamma$, as shown in Fig. 5 and both depend only on λ_1. We illustrate three different values of λ_1 allowed by tree-level unitarity and by $\mathrm{Br}(h \to gg)$ and $\mathrm{Br}(h \to \gamma\gamma)$ at 1σ. In each case we also indicate the effect of varying r_t in the range $r_t \in [-1, 1]$. We see that $h \to Z\gamma$ is less sensitive to both the color-octet scalars and the variations of r_t than $h \to \gamma\gamma$.

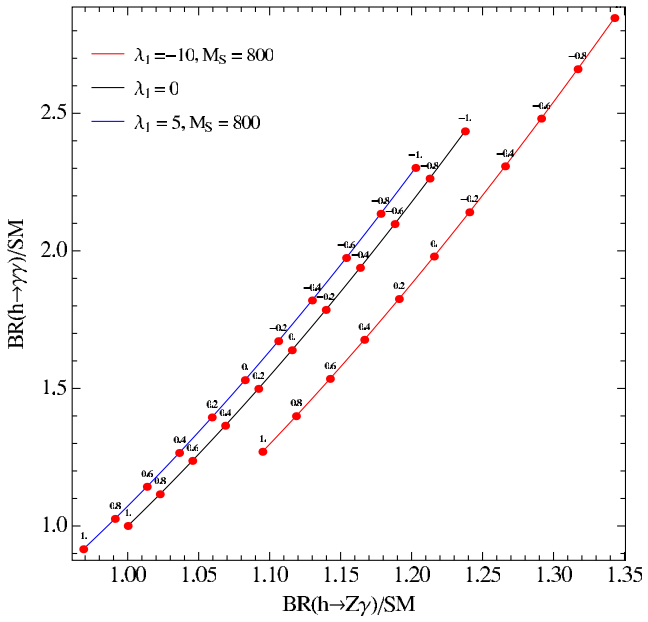

FIG. 5 (color online). Correlation between $\mathrm{Br}(h \to Z\gamma)$ and $\mathrm{Br}(h \to \gamma\gamma)$ for $M_S = 800$ GeV and three values of λ_1 as a function of r_t (indicated along the red dots).

VI. SUMMARY

The LHC has found a Higgs boson of mass near 126 GeV. The current available data have not yet pinpointed any of the Higgs couplings to fermions, the Yukawa couplings of the standard model. In this paper we have studied phenomenological constraints on the values of the top-quark Yukawa coupling to the observed Higgs boson. Data currently available to constrain this coupling comes from the one-loop Higgs boson amplitudes, namely its production via gluon fusion and its decay into two photons. The best fit value is away from the SM prediction although within the 1σ region. At 1σ, $0.8 \lesssim r_t \lesssim 1.2$ is allowed by the data.

We propose studying any deviation in terms of an interplay between new physics in the one-loop Higgs couplings and the top-quark Yukawa coupling. We have used a well motivated model, the color-octet model, to illustrate the effect of new particles contributing to the loop amplitudes. The color octet effects on these decays are already severely constrained from unitarity considerations, but they can still play a role in these modes. In particular they relax the allowed range (at 1σ) for the top quark–iggs coupling to $0.6 \lesssim r_t \lesssim 1.4$. We pointed out that both the color-octet scalars and the variations in r_t also play a role in $h \to Z\gamma$, although to a lesser extent.

Additional constraints on the top-quark Yukawa from Higgs-top associated production have also been recently investigated in [62–64], although at present they are significantly weaker.

ACKNOWLEDGMENTS

The work of X. G. H. and Y. T. was supported in part by NSC of ROC, and X. G. H. was also supported in part by the MOE Academic Excellent Program (Grant No. 102R891505) of ROC, and in part by the NNSF (Grant No. 11175115) and the Shanghai Science and Technology Commission (Grant No. 11DZ2260700) of PRC. The work of G. V. was supported in part by the DOE under Contract No. DE-SC0009974.

APPENDIX: HIGGS PRODUCTION AND DECAY

For completeness we review the main ingredients in the (leading-order) one-loop calculation of Higgs boson production in gluon fusion and its decay into two photons. For a general discussion BSM, we need to recall the different types of particles that can contribute to these two processes.

It is standard to parametrize the one-loop results with effective operators for hgg and $h\gamma\gamma$,

$$\mathcal{L}_{\mathrm{eff}} = c_g \frac{\alpha_s}{12\pi v} h G^a_{\mu\nu} G^{a\mu\nu} + c_\gamma \frac{\alpha}{\pi v} h F_{\mu\nu} F^{\mu\nu}. \quad \text{(A1)}$$

Different kinds of new particles such as a complex scalar S, a Dirac fermion f, and a charged and colorless vector V_μ that couple to the Higgs as

$$\mathcal{L} = -c_s \frac{2M_S^2}{v} hS^\dagger S - c_f \frac{M_f}{v} h\bar{f}f + c_V \frac{2M_V^2}{v} hV_\mu^\dagger V^\mu. \tag{A2}$$

contribute to the effective Higgs coupling to gluons and to photons as [65–68]

$$\delta c_g = \frac{3C_2(r_s)}{2} c_s A_s(\tau_s) + \frac{3C_2(r_f)}{2} c_f A_f(\tau_f), \tag{A3}$$

$$\delta c_\gamma = \frac{N(r_s)Q_s^2}{8} c_s A_s(\tau_s) + \frac{N(r_f)Q_f^2}{8} c_f A_f(\tau_f) - \frac{Q_V^2}{8} c_V A_V(\tau_V), \tag{A4}$$

where $\delta c_i = c_i - c_{i,\mathrm{SM}}$, $C_2(r)$ is the quadratic Casimir of the color representation r, and $N(r)$ is the number of colors of the representation r. The functions A_i are defined as

$$\begin{aligned} A_s(\tau) &\equiv \frac{1}{\tau^2}[f(\tau) - \tau], \\ A_f(\tau) &\equiv \frac{2}{\tau^2}[(\tau - 1)f(\tau) + \tau], \\ A_V(\tau) &\equiv \frac{1}{\tau^2}[3(2\tau - 1)f(\tau) + 3\tau + 2\tau^2], \\ f(\tau) &\equiv \begin{cases} \arcsin^2\sqrt{\tau} & \tau \le 1 \\ -\frac{1}{4}\left[\log\frac{\sqrt{\tau}+\sqrt{\tau-1}}{\sqrt{\tau}-\sqrt{\tau-1}} - i\pi\right]^2 & \tau > 1 \end{cases}, \end{aligned} \tag{A5}$$

with $\tau_i = m_h^2/4M_i^2$. The feature of $f(\tau) \simeq \tau + \frac{\tau^2}{3}$ when $\tau \simeq 0$, leads to $A_s(0) = \frac{1}{3}$, $A_f(0) = \frac{4}{3}$ and $A_V(0) = 7$.

In the physics BSM that we discuss in this paper, the only additional particles are scalars with $C_2(r_s) = 3$. The SM contribution through the top quark has $N(r_f) = 3$ and the octet has $N(r_s) = 8$. Deviations from the SM in the top-quark coupling are parametrized by $r_t = c_t$ in Eq. (A2) above. Since the masses of the color-octet scalars are not entirely due to the Higgs VEV, c_s are the ratio of the v^2-dependent mass term in M_s^2 to M_s^2, for instance, $c_{S^\pm} = (\lambda_1 v^2)/(4m_{S^\pm}^2)$.

In general, $hZ\gamma$ is also modified. Parametrized as $c_{Z\gamma}\frac{\alpha}{\pi v} hZ_{\mu\nu}F^{\mu\nu}$, we have [69–73]

$$\begin{aligned} c_{Z\gamma} = \frac{1}{8}\Big[& c_V Q_V^2 \cot\theta A_1^{Z\gamma}\left(\frac{1}{\tau_V}, \frac{1}{\lambda_V}\right) + c_f N(r_f)(2Q_f \cdot g_{Z\bar{f}f}) \\ & \times A_{1/2}^{Z\gamma}\left(\frac{1}{\tau_f}, \frac{1}{\lambda_f}\right) - c_s N(r_s)(2Q_S \cdot g_{ZSS}) \\ & \times A_0^{Z\gamma}\left(\frac{1}{\tau_S}, \frac{1}{\lambda_S}\right)\Big], \end{aligned} \tag{A6}$$

where $\lambda_i = \frac{M_Z^2}{4M_i^2}$. In the standard model, the top quark has $g_{Z\bar{f}f} = \frac{1-4Q_f\sin^2\theta_W}{2\sin\theta\cos\theta_W}$, and an octet scalar gives $g_{ZSS} = \frac{1-2\sin^2\theta_W}{2\sin\theta_W\cos\theta_W}$. Here θ_W is the Weinberg angle. The functions are defined as follows:

$$A_1^{Z\gamma}(x,y) = 4(3 - \tan^2\theta)I_2(x,y) + [(1 + 2x^{-1}) \times \tan^2\theta - (5 + 2x^{-1})]I_1(x,y), \tag{A7a}$$

$$A_{1/2}^{Z\gamma}(x,y) = I_1(x,y) - I_2(x,y), \tag{A7b}$$

$$A_0^{Z\gamma}(x,y) = I_1(x,y), \tag{A7c}$$

where

$$I_1(x,y) = \frac{xy}{2(x-y)} + \frac{x^2y^2}{2(x-y)^2}[f(x) - f(y)] + \frac{x^2y}{(x-y)^2}[g(x) - g(y)], \tag{A8a}$$

$$I_2(x,y) = -\frac{xy}{2(x-y)}[f(x) - f(y)]. \tag{A8b}$$

For $x > 1$ we have

$$f(x) = \arcsin^2\sqrt{1/x}, \tag{A9a}$$

$$g(x) = \sqrt{x-1}\arcsin\sqrt{1/x}. \tag{A9b}$$

For small changes, $\mathrm{Br}(Z\gamma)$ and $\mathrm{Br}(\gamma\gamma)$ are linearly correlated as

$$\frac{\mathrm{Br}(Z\gamma)/\mathrm{SM} - 1}{\mathrm{Br}(\gamma\gamma)/\mathrm{SM} - 1} = \left(\frac{\cos^2\theta_W - \sin^2\theta_W}{\cos\theta_W \sin\theta_W}\right) \times \frac{A_0^{Z\gamma}(\frac{1}{\tau_S}, \frac{1}{\lambda_S})}{A_0^{\gamma\gamma}(\tau_S)} \sqrt{\frac{\mathrm{Br}_{\mathrm{SM}}(\gamma\gamma)}{\mathrm{Br}_{\mathrm{SM}}(Z\gamma)}}.$$

[1] G. Aad *et al.* (ATLAS Collaboration), Phys. Lett. B **716**, 1 (2012).
[2] S. Chatrchyan *et al.* (CMS Collaboration), Phys. Lett. B **716**, 30 (2012).
[3] E. Farhi and L. Susskind, Phys. Rep. **74**, 277 (1981).
[4] T. Appelquist and M. S. Chanowitz, Phys. Rev. Lett. **59**, 2405 (1987); **60**, 1589(E) (1988).
[5] F. Maltoni, J. M. Niczyporuk, and S. Willenbrock, Phys. Rev. D **65**, 033004 (2002).
[6] A. V. Manohar and M. B. Wise, Phys. Rev. D **74**, 035009 (2006).
[7] R. S. Chivukula and H. Georgi, Phys. Lett. B **188**, 99 (1987).
[8] G. D'Ambrosio, G. F. Giudice, G. Isidori, and A. Strumia, Nucl. Phys. **B645**, 155 (2002).
[9] X.-G. He, H. Phoon, Y. Tang, and G. Valencia, J. High Energy Phys. 05 (2013) 026.
[10] W. Buchmuller and D. Wyler, Nucl. Phys. **B268**, 621 (1986).

[11] B. Grzadkowski, M. Iskrzynski, M. Misiak, and J. Rosiek, J. High Energy Phys. 10 (2010) 085.
[12] M. I. Gresham and M. B. Wise, Phys. Rev. D **76**, 075003 (2007).
[13] M. Gerbush, T. J. Khoo, D. J. Phalen, A. Pierce, and D. Tucker-Smith, Phys. Rev. D **77**, 095003 (2008).
[14] C. P. Burgess, M. Trott, and S. Zuberi, J. High Energy Phys. 09 (2009) 082.
[15] L. M. Carpenter and S. Mantry, Phys. Lett. B **703**, 479 (2011).
[16] T. Enkhbat, X.-G. He, Y. Mimura, and H. Yokoya, J. High Energy Phys. 02 (2012) 058.
[17] G. Cacciapaglia, A. Deandrea, G. D. La Rochelle, and J.-B. Flament, J. High Energy Phys. 03 (2013) 029.
[18] X.-G. He and G. Valencia, Phys. Lett. B **707**, 381 (2012).
[19] B. A. Dobrescu, G. D. Kribs, and A. Martin, Phys. Rev. D **85**, 074031 (2012).
[20] Y. Bai, J. Fan, and J. L. Hewett, J. High Energy Phys. 08 (2012) 014.
[21] I. Dorsner, S. Fajfer, A. Greljo, and J. F. Kamenik, J. High Energy Phys. 11 (2012) 130.
[22] G. D. Kribs and A. Martin, Phys. Rev. D **86**, 095023 (2012).
[23] J. M. Arnold and B. Fornal, Phys. Rev. D **85**, 055020 (2012).
[24] X.-G. He, G. Valencia, and H. Yokoya, J. High Energy Phys. 12 (2011) 030.
[25] J. Cao, P. Wan, J. M. Yang, and J. Zhu, arXiv:1303.2426.
[26] H. Flacher, M. Goebel, J. Haller, A. Hocker, K. Monig, and J. Stelzer, Eur. Phys. J. C **60**, 543 (2009); **71**, 1718(E) (2011).
[27] D. Carmi, A. Falkowski, E. Kuflik, and T. Volansky, J. High Energy Phys. 07 (2012) 136.
[28] A. Azatov, R. Contino, and J. Galloway, J. High Energy Phys. 04 (2012) 127; 04 (2013) 140(E).
[29] J. R. Espinosa, C. Grojean, M. Muhlleitner, and M. Trott, J. High Energy Phys. 05 (2012) 097.
[30] T. Li, X. Wan, Y.-k. Wang, and S.-h. Zhu, J. High Energy Phys. 09 (2012) 086.
[31] J. Ellis and T. You, J. High Energy Phys. 06 (2012) 140.
[32] A. Azatov, R. Contino, D. Del Re, J. Galloway, M. Grassi, and S. Rahatlou, J. High Energy Phys. 06 (2012) 134.
[33] M. Klute, R. Lafaye, T. Plehn, M. Rauch, and D. Zerwas, Phys. Rev. Lett. **109**, 101801 (2012).
[34] A. Azatov, S. Chang, N. Craig, and J. Galloway, Phys. Rev. D **86**, 075033 (2012).
[35] I. Low, J. Lykken, and G. Shaughnessy, Phys. Rev. D **86**, 093012 (2012).
[36] T. Corbett, O. J. P. Eboli, J. Gonzalez-Fraile, and M. C. Gonzalez-Garcia, Phys. Rev. D **86**, 075013 (2012).
[37] M. R. Buckley and D. Hooper, Phys. Rev. D **86**, 075008 (2012).
[38] M. Montull and F. Riva, J. High Energy Phys. 11 (2012) 018.
[39] J. R. Espinosa, C. Grojean, M. Muhlleitner, and M. Trott, J. High Energy Phys. 12 (2012) 045.
[40] D. Carmi, A. Falkowski, E. Kuflik, T. Volansky, and J. Zupan, J. High Energy Phys. 10 (2012) 196.
[41] S. Banerjee, S. Mukhopadhyay, and B. Mukhopadhyaya, J. High Energy Phys. 10 (2012) 062.
[42] D. Bertolini and M. McCullough, J. High Energy Phys. 12 (2012) 118.
[43] F. Bonnet, T. Ota, M. Rauch, and W. Winter, Phys. Rev. D **86**, 093014 (2012).
[44] T. Plehn and M. Rauch, Europhys. Lett. **100**, 11002 (2012).
[45] J. R. Espinosa, C. Grojean, V. Sanz, and M. Trott, J. High Energy Phys. 12 (2012) 077.
[46] G. Moreau, Phys. Rev. D **87**, 015027 (2013).
[47] E. Masso and V. Sanz, Phys. Rev. D **87**, 033001 (2013).
[48] T. Corbett, O. J. P. Eboli, J. Gonzalez-Fraile, and M. C. Gonzalez-Garcia, Phys. Rev. D **87**, 015022 (2013).
[49] G. Belanger, B. Dumont, U. Ellwanger, J. F. Gunion, and S. Kraml, J. High Energy Phys. 02 (2013) 053.
[50] C. Cheung, S. D. McDermott, and K. M. Zurek, J. High Energy Phys. 04 (2013) 074.
[51] K. Cheung, J. S. Lee, and P.-Y. Tseng, J. High Energy Phys. 05 (2013) 134.
[52] A. Falkowski, F. Riva, and A. Urbano, arXiv:1303.1812.
[53] B. Dumont, S. Fichet, and G. von Gersdorff, J. High Energy Phys. 07 (2013) 065.
[54] P. P. Giardino, K. Kannike, I. Masina, M. Raidal, and A. Strumia, arXiv:1303.3570.
[55] T. Alanne, S. Di Chiara, and K. Tuominen, arXiv:1303.3615.
[56] J. Ellis and T. You, J. High Energy Phys. 06 (2013) 103.
[57] A. Djouadi and G. Moreau, arXiv:1303.6591.
[58] W.-F. Chang, W.-P. Pan, and F. Xu, arXiv:1303.7035.
[59] A. Hayreter and G. Valencia, arXiv:1304.6976.
[60] ATLAS Collaboration, Report No. ATLAS-CONF-2013-034, "http://cds.cern.ch/record/1528170/files/ATLAS-CONF-2013-034.pdf".
[61] S. Chatrchyan *et al.* (CMS Collaboration), J. High Energy Phys. 05 (2013) 145.
[62] S. Biswas, E. Gabrielli, and B. Mele, J. High Energy Phys. 01 (2013) 088.
[63] M. Farina, C. Grojean, F. Maltoni, E. Salvioni, and A. Thamm, J. High Energy Phys. 05 (2013) 022.
[64] S. Biswas, E. Gabrielli, F. Margaroli, and B. Mele, arXiv:1304.1822.
[65] J. R. Ellis, M. K. Gaillard, and D. V. Nanopoulos, Nucl. Phys. **B106**, 292 (1976).
[66] B. L. Ioffe and V. A. Khoze, Fiz. Elem. Chastits At. Yadra **9**, 50 (1978) [Sov. J. Part. Nucl. **9**, 118 (1978)].
[67] M. A. Shifman, A. I. Vainshtein, M. B. Voloshin, and V. I. Zakharov, Yad. Fiz. **30**, 711 (1979) [Sov. J. Nucl. Phys. **30**, 1368 (1979)].
[68] A. Djouadi, Phys. Rep. **457**, 1 (2008).
[69] R. N. Cahn, M. S. Chanowitz, and N. Fleishon, Phys. Lett. **82B**, 113 (1979).
[70] L. Bergstrom and G. Hulth, Nucl. Phys. **B259**, 137(E) (1985); **B276**, 744 (1986).
[71] J. F. Gunion, H. E. Haber, G. L. Kane, and S. Dawson, Front. Phys. **80**, 1 (2000).
[72] A. Djouadi, V. Driesen, W. Hollik, and A. Kraft, Eur. Phys. J. C **1**, 163 (1998).
[73] C.-S. Chen, C.-Q. Geng, D. Huang, and L.-H. Tsai, Phys. Rev. D **87**, 075019 (2013).